Proceedings of BS2013:
13th Conference of International Building Performance Simulation Association, Chambéry, France, August 26-28

MULTI-CRITERIA GRID IMPACT EVALUATION OF HEAT PUMP AND PHOTOVOLTAIC BASED ZERO-ENERGY DWELLINGS

Ruben Baetens[1] and Dirk Saelens[1]

[1]KU Leuven Department of Civil Engineering, Building Physics Section,
BE-3001 Leuven, Belgium.

ABSTRACT

A multi-criteria evaluation of the impact on the electricity distribution grid in a residential built environment evolving towards nearly zero-energy is presented. A testbed is set up for the Belgian context with existing distribution grid topologies and urban planning. The latter is used for a Monte-Carlo simulation varying the degree of implementation of residential heat pump (HP) and photovoltaic (PV) systems.

Local technical feeder constraints consisting of possible transformer overload, impermissible voltage quality and voltage safety controls limits the possible penetration level before local feeder reinforcements are required: grid constraints are reached at penetration levels starting from 0.32, depending on local feeder design and sizing. While the integration of HP and PV based nearly zero-energy dwellings can reduced the average net electricity demand from 3 500 down to 530 kWh per houshold without facing technical constraints, the electrical energy losses in the feeder evolve from an average low 16 kWh to 323 kWh per household.

The impact of the urban design and geographical energy density on the one hand, and feeder typologies on the other hand on the voltage-related criteria will be researched in future work.

INTRODUCTION

The recent recast 2010/31/EU regarding European directive 2002/91/EC on building energy performance obliges all members to ensure that by 2020 ["all new buildings are nearly Zero-Energy.."] (The European Parliament, 2010). Although the definition of a nearly-zero energy building (ZEB) is unelaborated, the recast aims to combine energy efficiency with local renewable energy sources.

Non-simultaneity between local energy demand and supply, however, may strongly affect the power quality at electricity distribution feeder level and the load profiles at grid level. This impact limits the economic and energetic effectiveness of a widespred nearly-ZEBs implementation compared to an assessement at building level. The involved large scale integration will require well developed solutions in the form of energy storage and demand side management. Regarding the local low-voltage distribution grid at which the presented work focuses, the main consequences are summarized by Khator and Leung (1997): Steady-state voltage rises and drops potential result in curtail losses and appliance malfunction, while HP and PV integration can result in increased resistive grid energy losses. Furthermore, grid peak loads and potential transformer overloads and strong grid voltage and power flow fluctuations might occur at the point of common coupling.

The presented work quantifies the impact on the low-voltage distribution grid of a building stock evolving towards nearly-ZEBs. The assumption is made that this development is based on the implementation of heat pump (HP) and photovoltaic (PV) technologies as potential standard practice on the short to medium term. The latter stems from the current strong increase in HP and PV systems on the domestic market whereby these technologies may become standard practice in the short to medium term (European Heat Pump Association, 2009; EurObserv'ER, 2009).

The presented work distinguishes itself from the theoretical cases presented in earlier work (Baetens et al., 2012, 2011; De Coninck et al., 2013) by integrating the available data on the existing low-voltage feeder typologies and on the existing urban planning. Integrating both databases as a testbed for simulations allows defining a preliminary variation on the above stated impact on the low-voltage distribution grid. Based on this variation, an order-of-size on the local degree of implementation of residential nearly-ZEBs can be defined for which grid balancing technologies must start to play a role.

METHODOLOGY

A tool for Integrated District Energy Assessment Simulation (IDEAS) is developed earlier by Baetens et al. (2012) allowing transient simulation of thermal and electrical processes at neighborhood level. The latter is used for a set of simulations for the Flemish (Belgium) context varying the existing distribution grid topologies on the one hand, and the degree of implementation of nearly-ZEBs with HP and PV systems on the other hand. A total of 7 distribution islands have been simulated, denoting 21 feeders and 377 residential dwellings and an equal number of cases.

All simulations are performed for the typical moderate climate of Uccle (Belgium) and daylight saving time (DST) is taken into account. Irradiance data with a time resolution of 15 minutes are obtained by Meteonorm v6.1 for the moderate climate of Uccle (Belgium) (Meteotest, 2008) based on 1981-2000.

Figure 1: Graphical representation of the available data in the Distribution System Operator (DSO) Geographical Information System (GIS) databse [left] on the 0.4 kV *low-voltage distribution grid (black), the 10* kV *low-voltage distribution grid (black) and the 10/0.4-*kV *distribution transformers in between, and of the available data in the Flemish Agency for Geographical Information (Agiv) Geographical Information System (GIS) databse [right] on the known cadastral buildings and parcals for the same location.*

MODEL DESCRIPTION

The model description can be divided in three levels, ie. the mesoscale including grid typology and urban planning, the buildings and its thermal system and the occupant behavior and household load.

Mesoscale model description

Available data in a geographic information system (GIS) format for a given city and adjacent rural villages of the distribution system operator (DSO) on low-voltage grid typologies, and of the Flemish Agency for Geographical Information (Agiv) on urban planning are used as input data.

Grid typology

The DSO GIS database consist of the geographical toppolgy of the 0.4 kV-voltage and 10 kV mid-voltage grid, and the location of the transformers in between as shown in Figure 1.

Most occuring grid cables are of type EAXVB 1 kV 4 x 50 mm^2, type EAXVB 1 kV 4 x 75 mm^2, type EAXVB 1 kV 4 x 95 mm^2 or of type EAXVB 1 kV 4 x 150 mm^2. The line impedance values are presented in Table 1 and are calculated according design specifications in the Belgian standard NBN C33-322 (1975) for a grid frequency of 50 Hz. The present 10/0.4-kV distribution transformers have a nominal power of 160 kVA, 250 kVA or 400 kVA.

The junction cables between the supply terminal of each house and the distribution feeder are of type EXVB 1 kV 4 x 16 mm^2 and have a depicted length depending on the grid cables location known in the DSO GIS database and the dwelling location known in the Agiv GIS database. All dwellings are assumed to have a three-phase connection with the feeder resulting in a symmetric feeder load. The latter differs from existing distribution grids in the Belgian context consisting of single-phase connections between one phase and the neutral conductor with a nominal line-to-neutral voltage of 230 V, but the assumption on three-phase connections is justifiable in the future context of high HP and PV penetration levels.

Table 1: Overview of the main cable and transformer impedance values.

Cable type	Characteristic impedance
EXVB 4 x 16 mm^2	2.105 + j 0.076 Ω/km
EAXVB 4 x 50 mm^2	0.641 + j 0.073 Ω/km
EAXVB 4 x 75 mm^2	0.431 + j 0.072 Ω/km
EAXVB 4 x 95 mm^2	0.320 + j 0.072 Ω/km
EAXVB 4 x 150 mm^2	0.206 + j 0.070 Ω/km

Transformer type	Impedance
10/0.4-kV 120 kVA	0.014 + j 0.034 pu
10/0.4-kV 250 kVA	0.013 + j 0.038 pu
10/0.4-kV 400 kVA	0.009 + j 0.042 pu

Urban planning

The Agiv GIS database is an accurate reference map generally used as inventory of vacant lots and for building permit management consisting of the geographical toppolgy on all known cadastral buildings and parcals as shown in Figure 1.
The used data form the Agiv GIS databases consist of the building width and depth at the ground floor, the building orientation, the building typology (ie. a terrace, semi-detached or detached dwelling) and the orientation of the pitched roof if present. The latter is defined with visual inspection of aerial photography as additional information when in doubt. The retrieved parameters are used for resizing of predefined parametrized reference dwellign typologies and dimensioning of the maximum possible nominal power of the PV system based on the available roof area as decribed later on.
Overlaying the DSO GIS data with the Agiv GIS data allows the assignement of the buildings to their respective main distribution feeder, allowing to study the impact of urban planning and neighborhood design on possible grid restrictions as summarized in the introduction.

Buiding model description

The transient thermal building response model, the model dynamics of the hydronic heating system as well as the model for the domestic electricity system are described in succession for all dwellings.

Reference typologies

The implemented residential neighborhood are modeled based on 3 different architectural types, ie. a detached, semi-detached and terraced dwelling for which the main characteristics are listed in Table 2. All dwellings are modeled as a single-zone model for computational purposes and are parameterized based on their facade width, building depth and facade orientation for implantation in the neighborhood retrieved from the Agiv GIS database.
All dwellings in which a HP and PV system are applied are renovated to a low-energy standard as summarized in Table 2 for the reference typologies before scaling accoriding to urban planning data. Heat losses by conduction are reduced to a minimum by applying thermal insulation to obtain an overall mean heat transfer coefficient of 0.11 $\mathrm{W/m^2K}$, 0.13 $\mathrm{W/m^2K}$, 0.10 $\mathrm{W/m^2K}$ and 0.8 $\mathrm{W/m^2K}$ for the cavity walls, concrete foundation floors, timber roof constructions and windows respectively. Also ventilation losses are reduced to a minimum: all dwellings are as airtight as possible with a natural infiltration rate of 0.03 ACH. All dwellings are equipped with mechanically balanced, air-to-air heat-recovery ventilation (HRV) with an air change rate of 0.5 $\mathrm{h^{-1}}$ and a recovery efficiency of 0.84. Depending on the architectural types these measures result in a design heat load (EN 12831, 2003) of 20 to 28 $\mathrm{W/m^2}$ for the moderate climate of Uccle, Belgium.
Furthermore, all dwellings are equipped with exterior solar screens with a solar transmittance of 0.24 and the windows can be opened for natural ventilation. As a result no active cooling needs to be installed in the dwellings.

Hydronic heating system

All dwellings have a space heating (SH) and domestic hot water (DHW) system with an identical layout for each dwelling but different capacity, consisting of a modulating air-to-water heat pump (HP), thermal storage by means of a water buffer, a DHW temperature mixing valve and low-temperature radiators in each building zone. The nominal power of the heat production and emission system components are based on the design heat demand of the dwelling.
The storage tank of 0.35 $\mathrm{m^3}$ provides the DHW through a thermostatic mixing valve in order to obtain water at 45°C and is connected to the HP through an internal heat exchanger. The model of tank assumes 5 stratification layers and contains 2 temperature sensors for control purposes, ie. T_{top} and T_{bot} in the upper and 4th layer respectively. Heat losses of the insulated tank to the surroundings are included by a heat transfer coefficient of 0.4 $\mathrm{W/m^2K}$ and a static reference temperature of 15°C.
Space heating is performed by feeding low-temperature radiators with a design inlet and outlet temperature of 55°C and 45°C respectively at a design outdoor temperature of -8°C. The emission power is modeled with a radiative fraction of 0.35 and a radiator coefficient of 1.3.
The HP model is based on interpolation in a performance map retrieved from manufacturer data (Daikin Europe N.V., 2006). The interpolation defines the heating power Q_{net} and electricity use P_{net} as a function of condenser outlet temperature, the ambient temperature and can modulate to 30%. The coefficient of performance based on manufacturer data is 3.17 at 2/35°C test conditions (ie. air/water temperature) and 2.44 at 2/45°C test conditions for full load operation. The HP is controlled based on the measured and setpoint values for the storage tank temperatures T_{top} and T_{bot}. The HP control setpoints are based on a heating curve for SH (ie. 55°C at an outdoor temperature of -8°C and 20°C at an outdoor temperature of 15°C) and the required temperature for DHW of 45°C.
The control of the SH and DHW system is managed by a double control loop. The first loop controls the flow rate through the heat pump and the control signals to the pump towards the radiators and the pump towards the storage tank. The former signal is sent by the room thermostat based on the operative temperature, the setpoint and a dead band of 1°C around the setpoint. The latter signal is based on the measured and set point values for the storage tank top temperature T_{top}, measured in the second layer and a hysteresis of 2°C above setpoint is applied. The second loop controls the con-

Table 2: Model parameters for the reference detached, semi-detached and terraced dwelling typolgies.

Dwelling typologies		Detached	Semi-Det.	Terraced	
A_{heat}	Heated floor surface	260.0	196.0	118.0	m^2
V_{heat}	Heated volume	741.4	642.7	549.8	m^3
$\dot{V}_{inf}$	Infiltration rate	0.03	0.03	0.03	h^{-1}
$\dot{V}_{ven}$	Ventilation flow rate	0.50	0.50	0.50	h^{-1}
η_{hr}	Ventilation heat recovery efficiency	0.84	0.84	0.84	(-)
	Window-to-floor ratio	0.24	0.24	0.31	(-)
H_{tot}	Overall heat loss coefficient	132.9	100.8	73.3	$\mathrm{W/K}$
Φ_{design}	Specific building design heat load (for Ukkel, Belgium)	6 710	4 980	3 340	W

denser set temperature. A distinction is made based on which pump is running. When pumpFH is activated, the set point follows a heating curve for space heating, but with an offset of 2°C in order to compensate for distribution losses. When pumpDHW is activated, the set point is 5°C higher than the DHW tank set point in order to be able to reach the switch off condition on T_{top}.

Domestic electricity system model

Local renewable elektricity generation is provided by a building integrated photovoltaic (BIPV) system. All systems are assumed to be located on the roof surface oriented most South with an orientation-dependent inclination resulting in the highest annual electricity production (Huld and Suri, 2010). The BIPV systems are sized to cover 80% of the depicted roof surface. Calculations are based on manufacturer characteristics, ie. a maximum power point (mpp) current I_{mpp} of 6.71 A and mpp voltage V_{mpp} of 34.3 V, a short-circuit current I_{sc} of 7.22 A and an open-circuit voltage V_{oc} of 42.3 V at standard testing conditions. The temperature dependence is low with temperature coefficients k_i and k_v of 0.00217 and -0.106 respectively.

The direct current power output of the BIPV system is converted to an alternating current power by means of an inverter characterized by a constant inverter efficiency of 0.95. To avoid excessive feeder voltages, the BIPV system inverter is curtailed when the voltage at the dwellings feeder interface reaches a predefined voltage limit. This limit is set at an increase of 10% of the nominal feeder voltage or 253 V according to national regulations on AREI Art.§235, the Belgian General Regulations for Electrical Installations (AREI) and te General Regulations for Labour Protection (ARAB). The inverter control is given a minimal off-time of 5 min before trying to switch on again after voltage disturbances.

The nodal voltage of all appliances is set equal to the of the building-to-feeder connection. Furthermore, all electrical loads of the used appliances in the dwellings are seen as active loads P.

Occupant behavior

The stochastic behaviour of accommodated occupants concerning presence, the use of appliances and lighting, and domestic hot water draw-off are implemented as a combination of survival analyses for occupancy and embedded discrete-time Markov chains for the remainder.

Occupancy

Differently from earlier work (Baetens et al., 2012), occupancy is no longer described based on discrete-time Markov chains. The required differentiation based on household typologies results in a more comprehensive representation of occupancy behaviour at household level and a more realistic representation of the simultaneity of the resulting power demand for SH and DHW.

Four different family types have been defined based on the work of (Cheng and Steemers, 2011), ie. a young couple both working full time during weekdays and partly present in the weekend, a family of 4 persons of which one parent works part time, a non-working couple and a retired couple. For each family type, the average number of persons at home are defined for a typical weekday and a typical weekend from Aerts et al. (2013). In order to obtain fully stochastic profiles, an uncertainty is applied to the average arrival and departure times for each household and an uncertainty to the average arrival and departure times for each day of the week for the survival analysis. Both uncertainties are defined by a standard deviation $sigma$ of 1 hour compared to the family type average and household average respectively. This results in all different occupancy profiles, while the aggregated profiles by family type still reflect the typical days. The family types are distributed in the building stock independently of a possible existing correlation between the dwelling typology and household types.

The simulated active occupancy are used as direct input for thermostat settings, ie. 21°C when persons are present and active, and 16°C otherwise.

Household electricity load

The implemented stochastics are described earlier by Baetens et al. (2012) and are consistent with Richardson (2010) based on discrete-time Markov chains. The resulting outputs are activity of the building occupants, the use of appliances and the use of lighting, and depend solely on the house-

hold size, the present appliances and fixtures, whether it is a weekday or weekend day and global irradiances. Here, the use of appliances and lighting has a one- minute resolution. To generate statistically relevant profiles, bottom-up data concerning household size and installed appliances are used based on Belgian (FOD Economie, 2008) and European (Richardson, 2010) statistics on household sizes and appliance ownership rates respectively.

Domestic hot water

Also the DHW model needs special attention and must be modelled stochastically due to its increased importance on the final energy demand in low energy buildings. Both the tap profile and the total hot water consumption are of importance and are discussed below.
The tap profile is strongly related to the activity of the building users, requiring a model in accordance with the simulated occupancy and activity of the users. Herefore, four different draw-off categories have been defined, ie. a short and medium draw-off, a shower and a bath consistent with Jordan and Vajen (2001). For each category, the flow rate, total DHW volume and the average number of occurrences per day is fixed. Ten-minute proclivities are determined based on the occupancy and activity proclivities from (Richardson, 2010) for each category and consistent with the modeling approach in Widén (2009). The resulting stochastic profile for the DHW tap profile is achieved by discrete-time Markov chains based on a calibration scalar to end up with the desired average equivalent consumption per capita.
The average daily DHW consumption is rather an output than an input due to the stochastics but is for determining the proclivity functions. Concerning all simulated dwellings, the overal average consumption amounts 33.1 liter per day per person at 60°C which is consistent with multiple surveys reporting an average consumption of 30 $\mathrm{L/d}$ per person with a range between 10 to 80 $\mathrm{L/d}$ (Lechner, 1998).

RESULTS

An overview at feeder scale on the energetic performance of the simulated testbed evolving towards zero-energy based on HP and PV technology is presented in Figure 2. The *nearly-ZEB penetration level* κ_{zeb} is introduced for ease of reference, denoting the (local) fraction of dwellings renovated to the depicted low-energy standard based on HP and PV systems.
Here, two constraints must be denoted when studied in an integrated district energy perspective: (1) the net feeder energy balance doesn't equal the sum of the net building energy balances for each house individually as determined by a building energy simulation, while (2) load and voltage capacity constraints limits the number of tecnically feasible solutions. Local technical feeder constraints (i.e. transformer overload, voltage quality and system curtailing) limit the possible κ_{zeb} before local feeder reinforcements are required as shown in red in Figure 2: grid constraints are reached at κ_{zeb}-values starting from 0.32, depending on local feeder design and sizing as shown in Figure 2. Local constriants limit the possible average net energy feeder balance to a net consumption pf 530 kWh per household (p.h.), while most sensitive feeder designs can't reach a net consumption of 1 050 kWhp.h. and the strongest feeders are able to reach a net positve balance of 1 280 kWp.h. without facing constraints. Negelcting feeder constraints, an average net energy positive feeder balance of 1 060 kWhp.h. can be achieved for a κ_{zeb} equal to one, while a limit number of neighborhoods remain net energy consuming up to 610 kWhp.h. due to a shortage on available PV capacity.

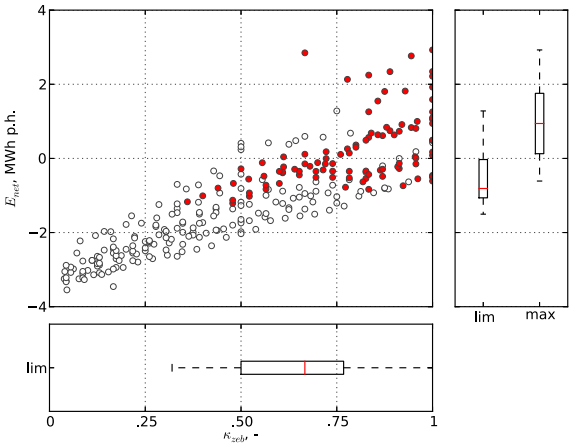

Figure 2: Resulting evolution of the net feeder energy balance E_{net} with increasing penetration level κ_{zeb} of HP and PV dwellings, denoting the technically feasible (white) and infeasible (red) solutions for existing feeder typologies. The (bottom) horizontal boxplot denotes the range in κ_{zeb} at which technical limits start to be a burden at feeder, whereas the (right) vertical boxplots show the range in net feeder energy balance E_{net} at the latter local technical limit κ_{zeb} and at a κ_{zeb} of unity.

DISCUSSION

Concerning building and district energy assessments, different trade-off indicators and criteria are of interest for different market parties: (1) households are concerned about their cost of ownership determined by the effective net energy balance E_{net} including the curtailed PV energy E_{cur} and possible discomfort, (2) distributions system operators are also interested in the resistive grid losses E_{Ω}, voltage quality and the transformer loads P_{tra} and (3) society is a third party which concerns about the net energy balance E_{cur} and the resulting equivalent carbon emissions $e_{\mathrm{CO_2}}$. In the presented work, the aforementioned interest for households are considered *on average* at feeder scale, to exclude the possible effect of micro-economic measures in the electricity price at high HP en PV penetration levels.

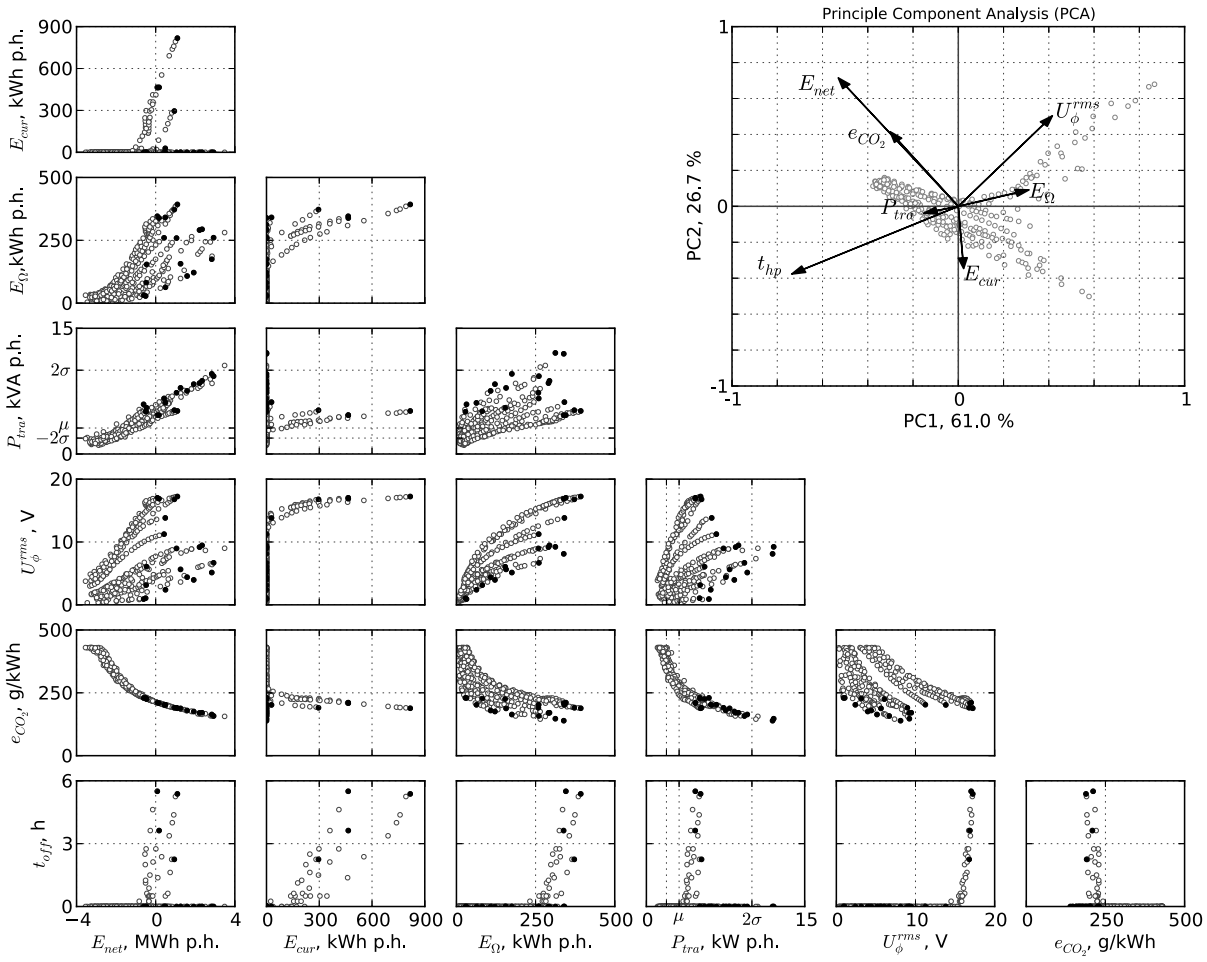

Figure 3: Trade-off grid impact criteria for the integration of HP and PV based zero-energy dwellings, ie. the net energy balance E_{net}, the line losses E_Ω, the transformer peak load P_{tra}, the characteristic feeder voltage deviation U_ϕ^{rms}, the specific emissions e_{CO_2}, the total disabled time of HP operating t_{off} and the total curtailed energy E_{cur}. Each dot represents a feeder design with variable degree of implementation for HP and PV systems, whereas the filled dots represent 100% integration of nZEBs at feeder level. The principle component analysis (PCA) of the grid impact objectives is presented at the top right including all situations plotted according to the first and second principle component PC1 and PC2. All energy-related objective functions are standardized per household (p.h.).

The latter trade-off criteria and their principle component analysis (PCA) as well as the integration of HP and PV based zero-energy dwellings are presented in Figure 3. A PCA rotates the set of criteria to align them with the directions of maximum variance. The x-axes of the PCA plot corresponds as such to the largest variance in critetria values and the y-axis to the second largest orthogonal variance. The denoted eigenvectors illustrate the direction of improvement of criteria values whereas the angle between vectors denote their linear correlation.

Ohmic losses

Distributions system operators (DSOs) are interested to minimize ohmic losses. Transporting electrical energy comes with resistive energy losses in the distribution lines and transformer, which can be determined as

$$E_\Omega = \sum_{\phi=1}^{n_\phi} \sum_{h \in \mathcal{H}_h} \int_k R_{\phi,h} \left| I_{\phi,k,h} \right|^2 \qquad (1)$$

where $R_{\phi,h}$ is the resistance of element h at phase ϕ, $I_{\phi,k,h}$ the electric current on timestep k in the depicted element and $\mathcal{H}_h$ the set of all resistive elements.

A trade-off can be denoted between the penetration level for HP and PV systems, and the annual ohmic losses E_Ω. Whereas the integration of PV systems is generally seen as causing a reduction of line losses up to a certain level, an overal increase of line losses is denoted here caused by the combined integration of HP systems. If a random integration of nearly-ZEBs based on HP and PV technology is considered, the average annual line losses will increase at higher penetration levels: considering all simulated feeders, the total resistive losses evolve quasi linearly from an average 16.5 kWhp.h. at the lowest penetration levels to

225.0 kWhp.h. for a κ_{zeb} equal to unity.
The dependency of E_Ω on the feeder resistances $[R_{\phi,h}]$ results in a large spread of $\pm 81\%$ on E_Ω with peak values up to 392.6 kWhp.h., as well as a positive correlation in $f : E_\Omega \mapsto U_\phi^{\text{rms}}$ as shown in Figure 3. The latter will be discussed later.

Voltage quality

DSOs are also interest to maximize the voltage quality, thus minimizing peak values concerning voltage regulation. Therefore, the characteristc daily voltage peak deviation U_ϕ^{rms} is defined as the root mean square value of all daily maximum peak deviations

$$U_\phi^{\text{rms}} = \sqrt{\frac{1}{n_d}\sum_{d=1}^{n_d} \max_{k \in \mathcal{K}_d} \left(|U_{\phi,k}| - U_{\text{nom}}\right)^2} \quad (2)$$

where U_{nom} is the nominal grid voltage, $U_{\phi,k}$ the voltage at the connection phase ϕ on timestep k, n_d the number of days in the evaluation period and $\mathcal{K}_d$ the set of timesteps in day d.
If a random integration of nearly-ZEBs based on HP and PV technology is considered, the average voltage quality will decrease at higher penetration levels: considering all simulated feeders, the characteristc daily voltage peak deviation U_ϕ^{rms} evolves quasi linearly from an average 2.2 V at the lowest penetration levels to 8.4 V for a κ_{zeb} equal to unity. Also here, the dependency of U_ϕ^{rms} on $[R_{\phi,h}]$ results in a large spread of $\pm 94\%$ on U_ϕ^{rms} with peak values up to 17.2 V, which are of higher importance than the averages.
Within a single feeder, a quasi-linear and quasi-quadratic relationship is found for $E_{\text{net}} \mapsto U_\phi^{\text{rms}}$ and $E_{\text{net}} \mapsto E_\Omega$ or $U_\phi^{\text{rms}} \mapsto E_\Omega$ respectively. The PCA shown upper-right in Figure 3 however shows that the main variance in voltage quality can not be attributed to the net energy balance E_{net} only. This finding denotes the importance of the design parameters $[R_{\phi,h}]$ taken into account in the modelling of the feeder typology and urban planning. The latter restricts the generalization of results retrieved by voltage quality optimization based on a single feeder design or neighborhood, and indicates the possibility or potential of feeder and urban planning optimization towards the integration of HP and PV systems from a DSOs' perspective.

Peak voltage measures

Peak voltages require PV curtailing if $U_{\phi,k}$ exceeds $1.1 \cdot U_{\text{nom}}$, whereas HP disfunctioning might occur when $U_{\phi,k}$ drops below $0.9 \cdot U_{\text{nom}}$. Curtailing losses E_{cur} as well as potential HP disfunctioning t_{off} occur only in respectively 5 and 4 out of the 21 simulated feeders: the reason can be found in the strong dependency of the voltages $U_{\phi,k}$ on the feeder resistances $[R_{\phi,h}]$ and the threshold value below which no curtailing is required. Both measures have effect on the individual household level but require solutions from the DSO.
PV curtailing losses E_{cur} are found starting from photovoltaic energy penetration levels κ_{pv} of 0.6 and reach up to 817.3 kWhp.h. for κ_{zeb} equal to unity, while HP curtailing times t_{off} start occuring from heat pump energy penetration levels κ_{hp} of 0.5 and reach up to 5.5 hours per year for κ_{zeb} equal to unity. From a society point of view, the average curtailed energy E_{cur} averages at 98.6 kWhp.h. for κ_{zeb} equal to unity for all simulated feeders.

Transformer peak loads

The integration of HP and PV systems results in increased peak loads to be transfered from or towards the mid-voltage grid by the transformer: considering all simulated feeders, the transformer peak load P_{tra} evolves from an average 1.1 kVAp.h. at the lowest penetration levels to 7.2 kVAp.h. for a κ_{zeb} equal to unity. The dependency of installed PV capacity results in a large spread of $\pm 51\%$ on U_ϕ^{rms} with a maximum of 12.0 kVAp.h.. The latter is expressed by a clear linear relationship $E_{\text{net}} \mapsto P_{\text{tra}}$ with a small spread, whereas this relationship is less clear in $\kappa_{\text{zeb}} \mapsto P_{\text{tra}}$.
The existing feeders have an average installed transformer capacity of 3.1 kVAp.h. with lower and upper extrema of 1.9 kVAp.h. and 10.0 kVAp.h.. The latter results in possible transformer overload starting from a κ_{zeb} of 0.3, allthough some feeders are able to reach a κ_{zeb} of unity without facing overload problems. The depicted transformer overload is as such the first bottleneck for a widespread HP and PV integration in existing feeder typologies.
A trade-off can be noticed in $P_{\text{tra}} \mapsto U_\phi^{\text{rms}}$: two clusters can be distincted in the simulated feeders denoting a group with high peak transformer loads P_{tra} but low characteristc daily voltage peak deviations U_ϕ^{rms}, and an opposite group with high characteristc daily voltage peak deviations U_ϕ^{rms} but low peak transformer loads P_{tra}. The latter distinction can be used in future optimization as both bottlenecks will require a different approach in proposing possible solutions. The same trade-off can be noticed in $E_{\text{cur}} \mapsto P_{\text{tra}}$ and $E_{\text{cur}} \mapsto U_\phi^{\text{rms}}$ where curtailing (as well as possible HP disfunction t_{off}) occurs at typical high U_ϕ^{rms} but low P_{tra}. Here, PV curtailing is not only a protective measure for peak voltage but also limits the transformer peak loads.

Equivalent carbon emissions

The unsimultaneity of plug and HP load demand on the one side and PV supply on the other side not necessarely makes a zero-energy neighborhood a zero-emission neighborhood. Assuming that the HP and PV implementation does not affect the embodied emissions of electricity redrawn from the mid-voltage grid, the equivalent carbon emissions e_{CO_2} evolves from the Belgian electricity generation system average430 g/kWh down to an average 190 g/kWh

for a κ_{zeb} equal to one. The increase in effective demand due to HP integration, however, results in a total net increas of electricity-related carbon emissions.

A parabolic relation can be noted in $E_{\text{net}} \mapsto e_{\text{CO}_2}$. The latter results from the mitigateing effect of installing more and more PV at feeder level concerning e_{CO_2} caused by decreaseing cover factors. The different PV capacity avalaible in the neighborhoods design also results in a rather large spread of 139 to 230 g/kWh for a κ_{zeb} equal to unity.

CONCLUSION

A multi-criteria evaluation of the impact on the electricity distribution grid of a residential built environment evolving towards nearly zero-energy is presented in this work. A testbed is set up for the Flemish (Belgium) context and climate with existing distribution grid topologies and urban planning for integrated transient district energy assessment simulations. The latter is used as boundary condition for a Monte-Carlo simulation varying the degree of implementation of residential heat pump (HP) and photovoltaic (PV) systems, identifying possible feeder bottlenecks.

Local technical feeder constraints consisting of possible transformer overload, impermissible voltage quality and voltage safety controls limits the possible penetration level before local feeder reinforcements are required: grid constraints are reached at penetration levels starting from 0.32, depending on local feeder design and sizing. Local constriants limit the possible average net energy feeder balance to -530 kWh per household (p.h.), while most sensitive feeder designs can't reach a net balance of -1 050 kWhp.h. and the strongest feeders are able to reach a net positve balance of 1 280 kWhp.h. without facing constraints.

Electrical energy losses in the feeder evolve from an average low 16 kWhp.h. to an average 323 kWhp.h. when all buildings have HP and PV systems, with extrema up to 1 210 kWhp.h. in weak feeders.

Concidering the neighborhood designs with feeder problems,: two clusters can be distincted in the simulated feeders denoting a group with high peak transformer loads P_{tra} but low characteristc daily voltage peak deviations U_{ϕ}^{rms}, and an opposite group with high characteristc daily voltage peak deviations U_{ϕ}^{rms} but low peak transformer loads P_{tra}. The latter distinction can be used in future optimization as both bottlenecks will require a different approach in proposing possible solutions. The effective impact of the urban design and geographical energy density on the one hand, and feeder typologies on the other hand on the voltage-related criteria will be researched in future work and included in the principle component analysis.

ACKNOWLEDGMENTS

The authors gratefully acknowledge the Research Foundation Flanders (FWO) and the KU Leuven Energy Institute (EI) for funding this research.

REFERENCES

Aerts, D., Minnen, J., Glorieux, I., Wouters, I., and Descamps, F. 2013. Defining occupancy profiles for user behaviour modelling. In *Submitted for publication in: BS2013*, page 8.

Baetens, R., De Coninck, R., Helsen, L., and Saelens, D. 2011. Integrated dynamic electric and thermal simulations for a residential neighborhood: Sensitivity to time resolution of boundary conditions. In *Proc. of the 12th Conf. of The International Building Performance Simulation Association*, pages 1745–1752, Sydney.

Baetens, R., De Coninck, R., Van Roy, J., Verbruggen, B., Driesen, J., Helsen, L., and Saelens, D. 2012. Assessing electrical bottlenecks at feeder level for residential net zero-energy buildings by integrated system simulation. *Applied Energy*, 96(Smart Grids):74–83.

Cheng, V. and Steemers, K. 2011. Modelling domestic energy consumption at district scale: A tool to support national and local energy policies. *Environmental Modelling & Software*, 26:1186–1198.

Daikin Europe N.V. 2006. Technical data Altherma ERYQ007A, EKHB007A / EXHBX007A, EKSWW150-300. Technical report.

De Coninck, R., Baetens, R., Saelens, D., Woyte, A., and Helsen, L. 2013. Rule-based demand side management of domestic heat pumps in zero energy neighbourhoods. *Journal of Building Performance Simulation (Submitted to:)*.

EN 12831 2003. *Heating systems in buildings - Method for calculation of the design heat load*.

EurObserv'ER 2009. Baromètre photovoltaïque / Photovoltaic barometer: 9 533.3 MWc dans l'EU / in the EU. *Systèmes solaires - Le journal de photovoltaïque*, 1:72–103.

European Heat Pump Association 2009. Outlook 2010 - European heat pump statistics. Technical report.

FOD Economie 2008. Bevolking - Private, grootte en collectieve huishoudens. Technical report.

Huld, T. and Suri, M. 2010. PVGIS, PV Estimation Utility.

Jordan, U. and Vajen, K. 2001. Influence of the DHW load profile on the fractional energy savings: A case study of a solar combisystem with TRNSYS simulations. *Solar Energy*, 69:197–208.

Khator, S. and Leung, L. 1997. Power distribution planning: a review of models and issues. *IEEE Transactions on Power Systems*, 12(3):1151–1159.

Lechner, H. 1998. Analysis of energy efficiency of domestic electric storage water heaters. Technical report, Directorate General for Energy (DGXVII) of the Commission of the European.

Meteotest 2008. METEONORM Version 6.1 - Edition 2009.

NBN C33-322 1975. *Kabels Voor Ondergrondse Aanleg, met Synthetische Isolatie en Versterkte Mantel (Type 1 kV)*.

Richardson, I. 2010. *Integrated high-resolution modelling of domestic electricity demand and low voltage electricity distribution networks*. PhD thesis, Loughborough University.

The European Parliament 2010. Directive 2010/31/EU of the European Parliament and of the Council of 19 May 2010 on the nergy performance of buildings (recast).

Widén, J. 2009. *Distributed Photovoltaics in the Swedish Energy System*. PhD thesis.